Electronic Supplementary Material (ESI) for ChemComm.
This journal is © The Royal Society of Chemistry 2022

Spatially confined magnesiothermic reduction induced uniform mesoporous hollow silicon carbide nanospheres for high-performance supercapacitors

Jianhua Hou *[a], Liang Fang [a], Xiaozhi Wang[a], Hong Gao*[b] and Guoxiu Wang*[b]

[a] School of Environmental Science and Engineering, Yangzhou University, Yangzhou 225000, PR China.

[b] Centre for Clean Energy Technology, School of Mathematical and Physical Sciences, Faculty of Science, University of Technology Sydney, City Campus, Broadway, NSW 2007, Australia.

* Corresponding author. E-mail addresses: jhhou@yzu.edu.cn, hong.gao@uts.edu.au, guoxiu.wang@uts.edu.au.

Experimental section

Materials.

1-Ethyl-3-methylimidazolium tetrafluoroborate ($EMIMBF_4$ > 99%), KOH and HCl are analytical quality and purchased from Jiangsu Guotai Super Power New Materials Co., Ltd. Formaldehyde, magnesium powder, CTAB (hexadecyl trimethyl ammonium bromide) and 3-aminophenol were bought from Sinopharm Chemical Reagent Co., Ltd.

Synthesis of mesoporous hollow carbon/silica spheres (MHS-SiO_2/C).

During the synthesis of (MHS-SiO_2/C), CTAB (0.55 g) and resorcinol (0.21 g) were suspended in a solution with 9 ml ethanol and 23 ml deionized water at 25℃. After resorcinol absolutely dissolved, ammonia solution (NH_4OH, 0.22 mL, ~25*wt.* %) was inserted and stirred for 10 min. Then add 0.29 mL of formaldehyde, let stand for a few minutes until it turned transparent and becomes an emulsion. After that, 1 ml of TEOS was added immediately, and the prepared solution was stirred at 25 °C for 24 h, then heated in Teflon lined autoclave at 80 °C for another 24 hours. The solid product was produced by centrifugation and freeze drying. MHSs-C/SiO_2 composites were obtained by annealing the solid product at 800 °C for 2.5 h with a ramp rate of 1.5 °C min^{-1} in N_2 atmosphere. Furthermore, excess silica was eliminated by 10% HF solution for 24 h, thus mesoporous hollow carbon spheres (MHS-C) were produced. The MHS-C/SiO_2 composites were calcined at 600 °C for 6 h in air to produce the mesoporous hollow silica spheres.

Magnesiothermic reduction (MR) technology prepares mesoporous hollow SiC nanospheres (MHS-SiC).

MHS-SiC material was synthesized by the interfacial interaction of SiO_2 and carbon during MR process. A specific quantity of MHS-SiO_2/C and pure magnesium powders were mixed and placed into a ceramic, which was subsequently transferred to a tube furnace in argon atmosphere. With a ramp of 5 °C min $^{-1}$, the furnace was heated to 620 °C and maintained for 3.0 h. The acquired sample was then collected after returning to room temperature in a pure argon atmosphere. To get eliminate the by-product MgO from the sample, pure water and 1.0 M HCl solution were utilized. The 5 wt% HF solution was used to eliminate the unreacted SiO_2. The resulting sample was subsequently purified, cleaned with deionized water, and dried under vacuum at 110 °C. This as-prepared product is known as MHS-SiC.

Characterization.

Field emission scanning electron microscopy (FESEM) and Transmission electron microscopy (TEM) examinations were carried out using the Hitachi S-4800, Tecnai G2 F30 S-Twin. PANalytical-X-pert diffractometer (Cu K radiation at 40mA and 40kV) was used to detect powder X-ray diffraction (XRD) patterns (10-80° in 2θ). On a Malvern Zetasizer NanoZS instrument, dynamic light scattering (DLS) parameters were determined. For the XPS examination, an Axis Ultra spectrometer was employed. Micromeritics-ASAP-2020 was used to measure the nitrogen adsorption-desorption isotherm at 77K and relative pressure p/p_0 of 1.2 ×10 $^{-6}$ -0.990. Test samples were degassed at 250 °C for at least 4 hours before to the measurement. Pore size distribution and specific surface area (S_{BET}) were determined by density functional theory (DFT) calculations and Brunauer-Emmett-Teller (BET) measurements.

Electrochemical measurements.

The electrochemical characteristics of MHS-SiC were investigated in both $EMIMBF_4$ and 6 M KOH electrolytes. The electrodes were prepared by mixing MHS-SiC (86 wt. %), PTFE binder (4 wt. %) and acetylene black (10 wt. %). The EDLC current collectors were stainless steel (6 M KOH electrolyte) and aluminium mesh ($EMIMBF_4$ electrolyte) with 5-7 mg/ cm^2 electrode materials. Subsequently, the electrodes were vacuum-dried at 110°C for 8 hours. And polypropylene membrane was selected as separator. The cyclic voltammetry (CV), galvanostatic charge/discharge, and AC impedance spectroscopy (EIS) were measured through the CHI660E electrochemical workstation. With a 5 mV voltage amplitude, impedance spectra were measured in frequency range of 0.01 Hz–10 kHz. The capacitor's cutoff charge voltage of 6 M KOH solution was set to 0-1.0 V, while the cutoff charge voltage of $EMIMBF_4$ solution was 0-3.5 V.

Equation (1) was used to determine the specific capacitance for a single electrode.

$$c_g = \frac{2I}{(dV/dt)m} \qquad (1)$$

Where dV/dt(V/s) = slope of a discharge curve, m(g) = single electrode active material mass, and I(A) = discharge current. P_{cell} (specific power density) and E_{cell} (specific energy density) calculations were also evaluated for symmetrical supercapacitors, which are mentioned in the equation (2) and (3).

$$P_{cell} = \frac{E_{cell}}{t} \qquad (2)$$

$$E_{cell} = \frac{C_g \Delta V^2}{8 \times 3.6} \qquad (3)$$

Here, t(h), and ΔV(V) represented the discharge time and cell voltage after ohmic drop, respectively.

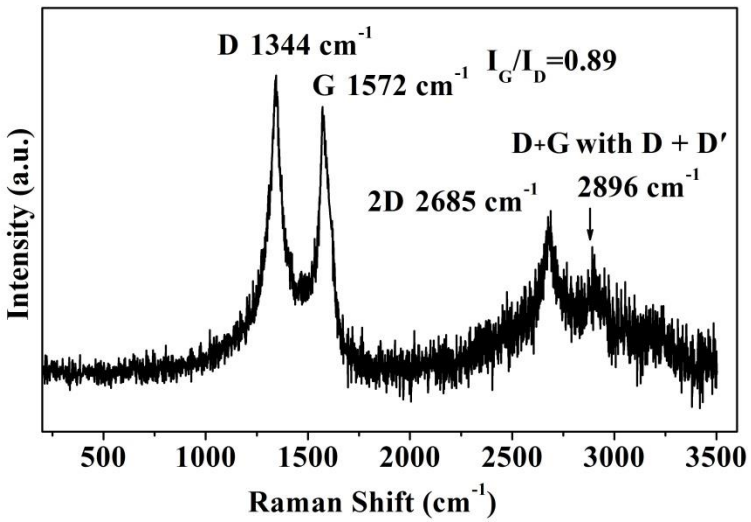

Fig. S1. Raman spectrum of MHS-SiC.

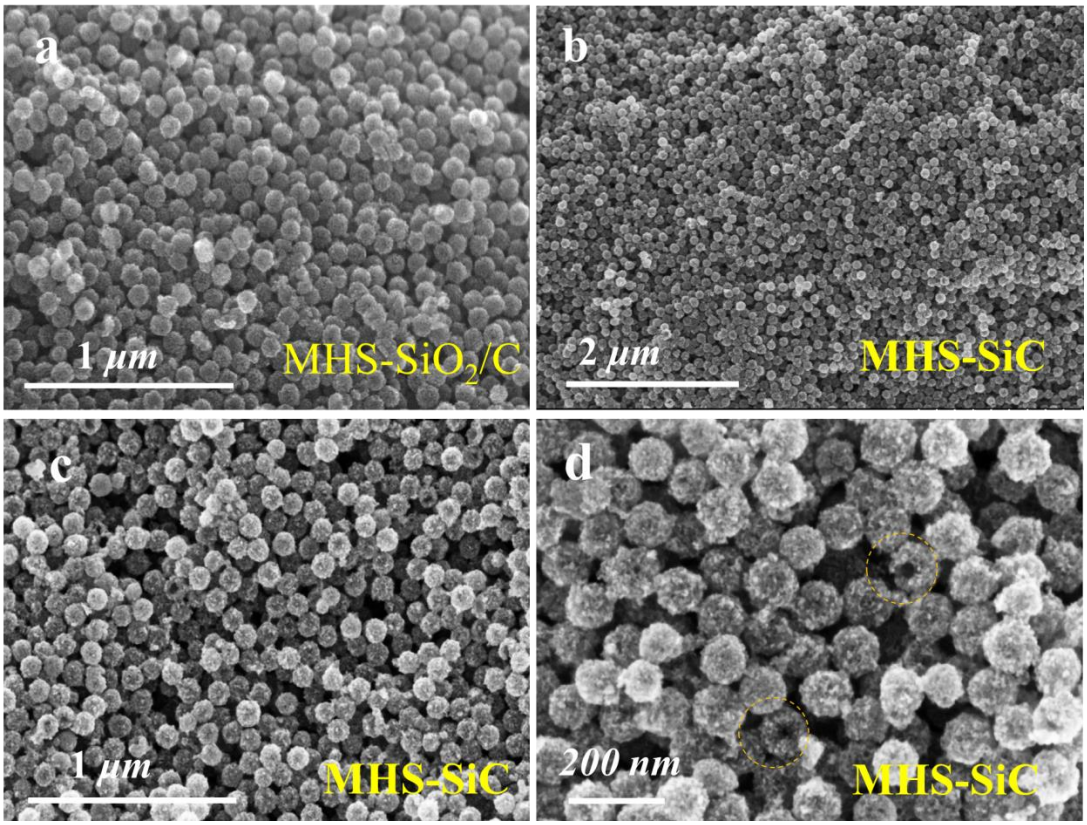

Fig. S2. (a) SEM images of MHS-SiO_2/C, (b, c,d) SEM images of MHS-SiC, the marked circles show the hollow structures.

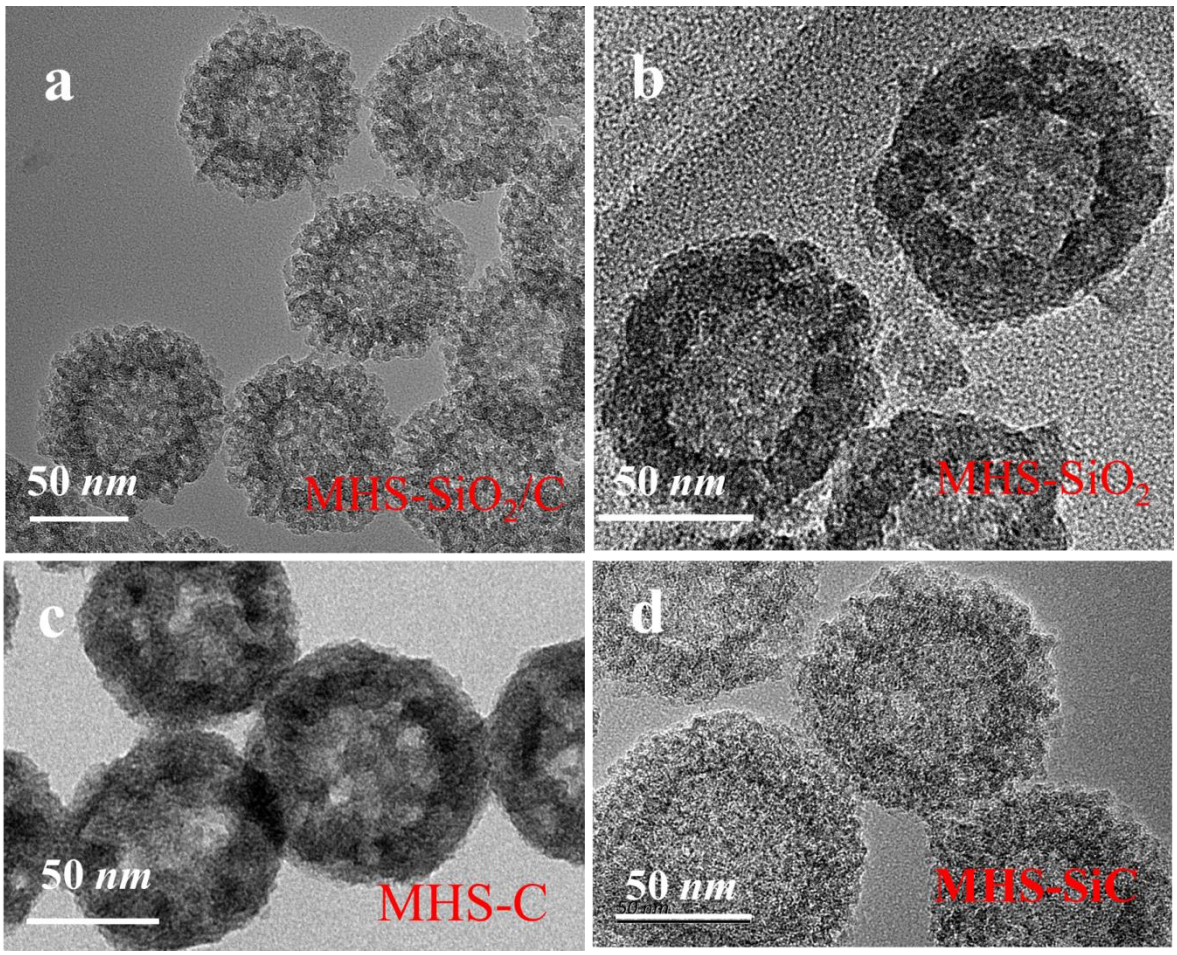

Fig. S3. TEM images of (a) MHS-SiO_2/C, (b) MHS-SiO_2, (c) MHS-C and (d) MHS-SiC.

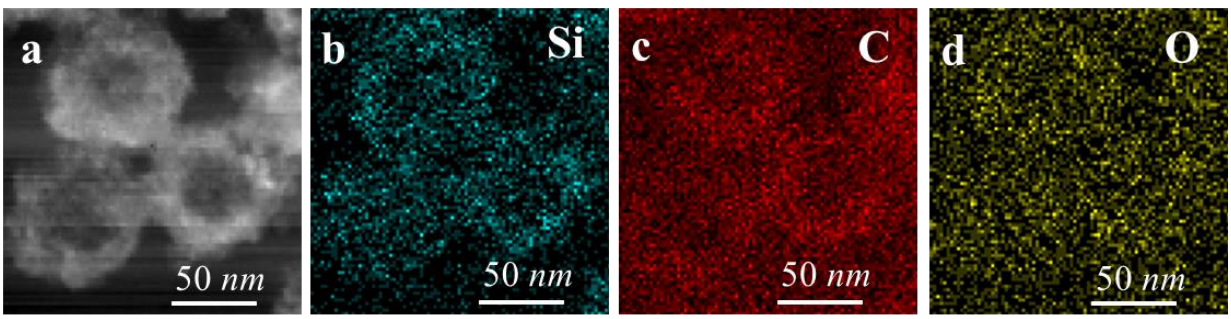

Fig. S4. (a) STEM, and corresponding (b-d) elemental mapping images of MHS-SiC

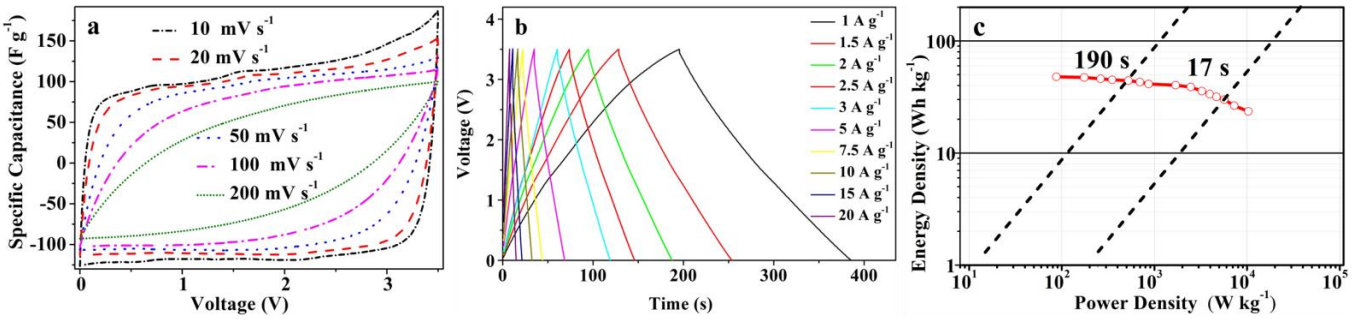

Fig. S5. (a) Cyclic voltammetry curves, (b) Galvanic charge-discharge curves, (c) Ragone plot of MHS-SiC in ionic liquid $EMIMBF_4$ electrolyte.

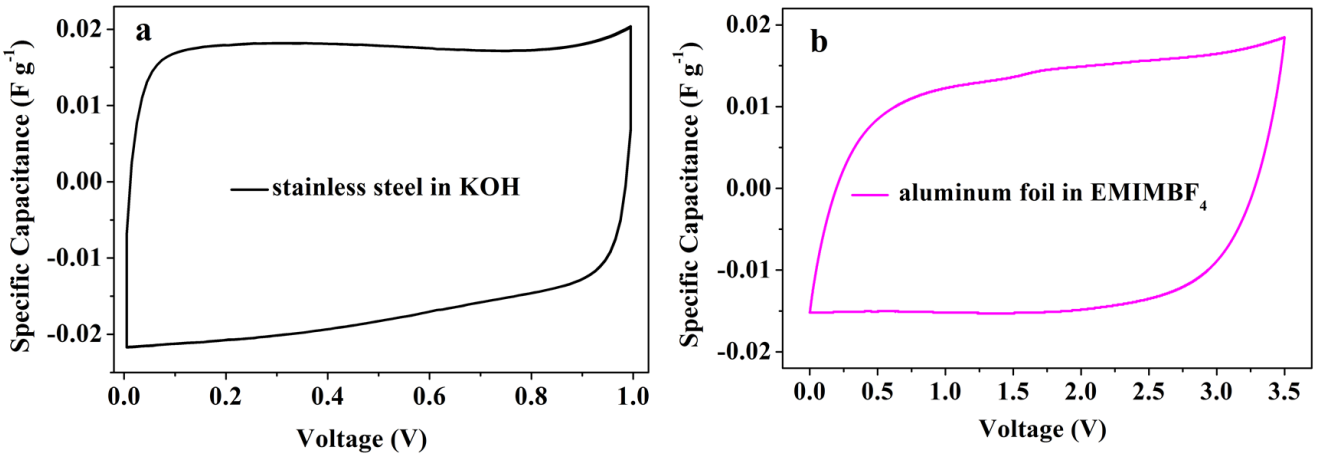

Fig. S6. (a) Cyclic voltammetry curves of stainless steel in KOH and aluminum foil in $EMIMBF_4$ electrolyte at a scan rate of 0.1 V s^{-1}.

Table S1. Comparison of specific surface area, pore volume and specific capacitance of the obtained **MHS-SiC** sample with previously reported samples.(a is a two-electrode system, and b is a three-electrode system)

Materials	S_{BET} (m^2 g^{-1})	Pore volume (cm^3 g^{-1})	Capacitance (F g^{-1})	Current density	Electrolyte	Ref.
Mesoporous Hollow SiC Nanospheres (MHS-SiC)	**868**	**1.49**	**134** **116** **114** **86**	**0.1 A g^{-1}** **100 A g^{-1}** **0.1 A g^{-1}** **20 A g^{-1}**	**6 M KOH** **EMIMBF$_4$**	**This work[a]**
silicon-oxy-carbide (SiOC)	5.64		102.3 66.8	5 mA g^{-1}	1 M Li_2SO_4 1 M $TEABF_4$	1[a]
SiC nanowires	-	-	29.5	0.25 A g^{-1}	2 M KCl	2[b]
Silicon Carbide Nanocauliflowers	-	-	72 41	1.43 A g^{-1} 0.71 A g^{-1}	1 M Na_2SO_4	3[a]
ordered mesoporous SiC@C	757.4	-	194.8 123	0.2 A g^{-1} 5 A g^{-1}	6 M KOH	4 [b]
SiC/C nanosheets			130 69	10 mV s^{-1} 0.5V s^{-1}	1 M Na_2SO_4	5[b]
SiC nanowire-derived carbon	1182	-	200 95	2 A g^{-1} 10 A g^{-1}	6 M KOH	6[a]
porous carbon/ silicon carbide	1357.9	0.76	234.2 167.3	1 A g^{-1} 20 A g^{-1}	1 M Na_2SO_4	7[b]
boron-doped SiC thin film on silicon		-	232 198 116	2.2 A g^{-1} 2 mV s^{-1} 80 mV s^{-1}	1 M H_2SO_4	8[b]
SiCNWs@ $NiCo_2O_4$NCs	55.4		131 72	1 A g^{-1} 20 A g^{-1}	PVA–KOH	9[a]
C doped SiC	1789		162 102	0.5 A g^{-1} 10 A g^{-1}	PVA-H_2SO4	10[a]

References

1 P. Pazhamalai, K. Krishnamoorthy, S. Sahoo, V. Mariappan, S. Kim, *Chem. Eng. J.*, 2020, **387**, 123886.

2 X. Li, W. Li, Q. Liu, S. Chen, L. Wang, F. Gao, G. Shao, Y. Tian, Z. Lin, W. Yang, *Adv. Funct. Mater.*, 2021, **31**, 2008901.

3 A. Sanger, A. Kumar, A. Kumar, P. Jain, Y.r Mishra, R. Chandra, Ind. Eng. Chem. Res. 2016, **55**, 9452-9458.

4 X. Liu, H. Zhao, S. Jiang, S. Wu, T. Zhao, L. Li, X. Geng, H. Yang, W. Zhou, C. Sun, Y. Chen, B., *J. Alloy. Compd.*, 2021, **881**, 160442-160450.

5 S. Liu, E.Wang, S.Liu, C. Guo, H.Wang, T.Yang, X. Houa, *J. Mater. Sci. Technol.*, 2022, **110**, 178-186.

6 X. Zou, L. Ji, H. Hsu, K. Zheng, Z. Pang, X. Lu, *J. Mater. Chem. A*, 2018, **6**, 12724-12732.

7 Q. Tang, X. Chen, D. Zhou, C. Liu, *Colloids Surf. A Physicochem. Eng. Asp.*, 2021, **620** , 126567-126576.

8 K. Kundu, A. Ghosh, A. Ray, S. Das, J. Chakraborty,S. Kumar, N. Prasad, R. Banerjee, *J Mater Sci: Mater Electron*, 2020, **31**,17943-17952.

9 X. Yin, H. Li, R. Yuan, J. Lu, *J. Colloid Interf. Sci.*, 2021, **586**, 219-232.

10 S.C. Abbas, C. Lin, Z. Hua, Q. Deng, H. Huang, Y. Ni, S. Cao, X. Ma, *Chem. Eng. J.*, 2022, **433**, 133738.